Accepted Manuscript

Self-stacking of exfoliated charged nanosheets of LDHs and graphene as biosensor with real-time tracking of dopamine from live cells

Ayesha Aziz, Muhammad Asif, Muhammad Azeem, Ghazala Ashraf, Zhengyun Wang, Fei Xiao, Hongfang Liu

PII: S0003-2670(18)31210-8

DOI: 10.1016/j.aca.2018.10.008

Reference: ACA 236314

To appear in: *Analytica Chimica Acta*

Received Date: 21 April 2018

Revised Date: 13 September 2018

Accepted Date: 8 October 2018

Please cite this article as: A. Aziz, M. Asif, M. Azeem, G. Ashraf, Z. Wang, F. Xiao, H. Liu, Self-stacking of exfoliated charged nanosheets of LDHs and graphene as biosensor with real-time tracking of dopamine from live cells, *Analytica Chimica Acta* (2018), doi: https://doi.org/10.1016/j.aca.2018.10.008.

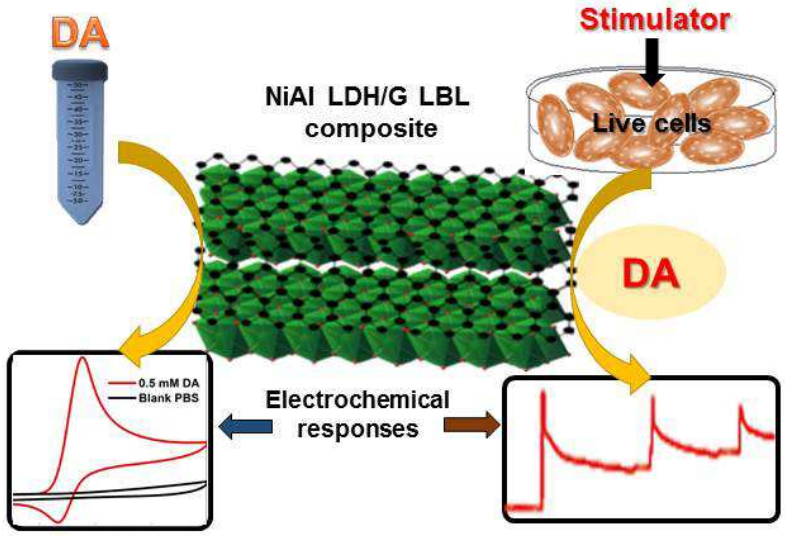

TOC

Self-stacking of exfoliated charged nanosheets of LDHs and graphene as biosensor with real-time tracking of dopamine from live cells

Ayesha Aziz[a], Muhammad Asif[a], Muhammad Azeem[b], Ghazala Ashraf[a], Zhengyun Wang[a], Fei Xiao[a], Hongfang Liu[a]*

[a] Key Laboratory for Large-Format Battery Materials and System, Ministry of Education, Hubei Key Laboratory of Material Chemistry and Service Failure, School of Chemistry and Chemical Engineering, Huazhong University of Science and Technology, Wuhan, 430074, P. R. China.

[b] School of Physics, Huazhong University of Science and Technology, Wuhan 430074, China.

Abstract

This study introduces a new strategy for periodic stacking of positively charged NiAl layered double hydroxides (LDHs) nanosheets with negatively charged monolayers of graphene (G) by systematically optimizing several parameters in a controlled co-feeding fashion and resultant heterostacked NiAl LDH/G LBL nanocomposites have been practically applied in sensitive detection of dopamine released from live cells as early Parkinson's disease (PD) diagnostic tool. PD is the second most chronic neurodegenerative disorder with gradual progressive loss of movement and muscle control causing substantial disability and threatening the life seriously. Unfortunately majority of dopaminergic neurons present in substantia nigra of PD patients are destroyed before it is being clinically diagnosed, so early stages PD diagnosis is essential.

Because of direct neighboring of extremely conductive graphene to semiconductive LDHs layers, enhanced intercalation capability of LDHs, and huge surface area with numerous active sites, good synergy effect is harvested in heteroassembled NiAl LDH/G LBL material, which in turn shows admirable electrocatalytic ability in DA detection. The interference induced by UA and AA is effectively eliminated especially after the modifying the electrode with Nafion. The outstanding electrochemical sensing performance of NiAl LDH/G LBL modified electrode has been achieved in terms of broad linear range and lowest real detection limit of 2 nM (S/N=3) towards DA oxidation. Benefitting from superior efficiency, biosensor has been successfully used for real-time *in-vitro* tracking of DA efflux from live human nerve cell after being stimulated. We believe that our biosensing platform of structurally integrated well-ordered LBL heteroassembly by inserting graphene directly to the interlayer galleries of LDHs material will open up new avenue in diseases determination window.

Keywords optimized co-feeding methodology, NiAl LDH/G LBL nanocomposites, electrochemical biosensor, DA detection, live nerve cells

1. Introduction

Dopamine (DA) as one of the extensively studied monoaminergic neuroreceptors which functions as chemical messenger in synaptic communication between cells, plays a vital role in cardiovascular modulation, control of stress responses in renal systems [1, 2] and various aspects of brain circuitry in living organisms [3, 4]. Owing to the co-existence of various biological molecules in human body, constructing an extremely accurate and ultra-sensitive method for precise monitoring of DA is incredibly important for clinical diagnosis, pathological analysis and

to be conscious of neuronal function [5]. To date, among the several analytical approaches [6, 7], electrochemical transducer based methods being low cost, sensitive and portable, [8, 9] have widely been used for real-time detection of DA since they hold certain intriguing abilities of selectivity, ease of operation, swift response and ultrasensitivity in biological systems [10].

It is worth mentioning that electrochemical response intensities are greatly influenced by material composition as well as surface properties of working electrode. In addition, it is challenging to exclude the influence of interfering species such as ascorbic acid (AA) and uric acid (UA) with almost same oxidation potential and high concentrations of AA together with DA in extracellular fluids [11]. Concerned with these consequences, electrochemical biosensors based on tailored nanocomposites and biological recognition species such as noble metal/oxides/hydroxides, and carbon based materials have been presented for DA sensing with improved sensitivity and selectivity [12, 13]. At bare electrodes, DA and AA are oxidized at similar potential giving overlapped peak and feeble response in DA detection [14]. To circumvent these bottlenecks, modified electrodes could be capable to avoid interference reactions and encourage DA oxidation through effective electrocatalytic reactions [15] and specific electrostatic interactions. Though, the noble metals being highly expensive and scarce as well as natural enzymes which are extremely instable, easily be denatured and complex while immobilizing [16, 17] have rendered their practical implementation in electrochemistry. Therefore, there is an urgent need of highly efficient electrocatalyst composed of inexpensive non-noble metals having conductive surfaces that should be characterized by the properties of high versatility in shape and size, surface regeneration, provide suitable mechanic and conducting characteristics, marvelous catalytic. Undoubtedly, nonprecious *3d* metal

oxides/hydroxides have exposed tremendous electrocatalytic properties owing to huge surface area, good stability and decent capability in electro catalysis systems [18].

Layered double hydroxides (LDHs), a class of inorganic materials with tunable heterogeneous metal cations and interlayer space offering the availability of anion exchange within the interlayer gallery, have been used as a superb working electrode material in electro catalysis, [19] separation [20] and biosensor platform [21]. Single layer macromolecular arrangement of LDH crystals by exfoliation is one of the fascinating characteristics of LDH, ultimately constructing 2D assembly of cationic nanosheets [22, 23]. Actually, the insulating behavior of these non-noble (Fe, Co, Ni, Mn, Zn) metal oxides/hydroxides has constrained LDH based proficient electro catalytic nanomaterials [24]. To circumvent these issues, molecular level hybridizing of single layer of very thin LDH nanosheets together with monolayers of some super conductive carbon materials such as conductive polymers or graphene (G) could be a perfect methodology to develop an electrode material with remarkable electrochemical performances. Unambiguously, graphene having large surface area and superior electrical conductivity could function as conductive pathways to improve catalytic efficiency. Probably, an enhanced synergistic effect and quick electron transferring efficiency would be expected if periodic stacking of cationic LDH nanosheets with negatively charged graphene monolayer in an alternate manner could be achieved as superlattice composite. To the best of our knowledge, there is no report on successful use of NiAl LDH/G LBL (layer by layer) hybrid composite in biosensing platform.

Herein, we report structurally hybridized composite material by controllable co-feeding methodology to yield heterostacked LBL self-assembly of NiAl LDH/G as shown in Fig. 1. Unequivocally, the confirmations about the construction of stacked NiAl LDH/G LBL hybrid

material are provided by various characterization techniques. Additionally, to circumvent the coagulation or destruction of structure, our structurally hybridized composite material NiAl LDH/G LBL can be recovered by freeze drying method in comparison with some above mentioned studies which could only use superlattice nanocomposites in wet conditions [25, 26]. As a proof of concept, NiAl LDH/G LBL modified electrode has demonstrated admirable electrochemical sensing performances and has been practically used for *in vitro* monitoring of DA efflux in live human nerve cells.

2. Experimental section

2.1. Reagents and materials

Sinopharm Group Chemical Reagent Co, Ltd. (Shanghai, China) was selected to get $Ni(NO_3)_2 \cdot 6H_2O$, $Al(NO_3)_3 \cdot 9H_2O$, Na_2CO_3, glucose, hydrogen peroxide (H_2O_2), urea, dopamine (DA), ascorbic acid (AA), uric acid (UA), 0.75% Nafion, Dulbecco's modified eagle's medium (DMEM) medium for cell culturing, highly concentrated K^+ buffer solution to encourage DA secretions from live cells and natural graphite. All these reagents were used without further purifications. Supporting electrolyte of 0.1 M phosphate buffer solution (PBS, pH=7.4) was used during the whole electrochemical assays. Typically 0.1 M solution of Na_2HPO_4 was prepared by dissolving 35.8 g of it into 1000 ml of doubly distilled (DD) water and 0.1 M solution of NaH_2PO_4 by dissolving 3.9 g of it into 250 ml of DD water. Then finally, 810 ml of 0.1 M Na_2HPO_4 and 190 ml of 0.1 M NaH_2PO_4 were mixed according to 81/19 proportion and pH was adjusted. X-ray diffraction (XRD) was carried out on a Rigaku D/max-r A diffractometer (Japan) using Cu Ka radiation (40 kV, 200 mA) with a Ni filter, X-ray photoelectron spectroscopy (XPS)

was done on an ESCALAB MKII spectrometer (VG Co., UK), using Mg Ka radiation (1253.6 eV) at a pressure of 2.0×10-10 mbar and Field-emission scanning electron microscope (FSEM) was acquired on HITACHI X-650 FSEM (Hitachi Co., Japan). Transmission electron microscopy (TEM) and high-resolution transmission electron microscopy (HRTEM) images were captured by TECNAI G220 U-Twin instrument (Netherlands). The whole electrochemical measurements were performed on CHI760 electrochemical workstation (CH Instrument Company, Shanghai, China) fitted with reference, counter and working electrode as saturated calomel electrode, platinum wire and glassy carbon electrode in typical three electrode system. All the electrochemical measurements were carried out at room temperature as well as in deoxygenated 0.1 M PBS (pH=7.4).

2.2. Cell culturing and real-time tracking of DA secretions

The human neuronal cell line (SH-SY 5Y) that functions as dopaminergic markers was received from the American Type Culture Collection (ATCC, Manassas, VA, USA). The cell line was cultured in DMEM, provided with 10% Fetal Bovine Serum (FBS), 100 units mL^{-1} penicillin and 100 mg mL^{-1} streptomycin and incubated at 37°C, 5% CO_2 with continued various passages. After completing few passages, the cells were seeded in 6-well plate with 80% confluency for real-time tracking of extracellular DA secretions. The working glassy carbon electrode (GCE) modified with NiAl LDH/G LBL superlattice nanohybrid (NiAl LDH/G LBL/GCE) was equipped very near to seeded cells in 6-well plate at 37°C for the detection of DA flux in neuronal cells after being released by the inoculation of highly concentrated K^+ buffer solution as stimulus [3].

2.3. Preparation of NiAl LDH

Powdered material of NiAl LDH with CO_3^{2-} inter gallery ions was fabricated by hydrothermal treatment according to our prior studies [27]. Briefly, a solution containing 6 mM $Ni(NO_3)_2 \cdot 6H_2O$, 2 mM $Al(NO_3)_3 \cdot 9H_2O$ and 24 mM urea was mixed together and transferred to Teflon-lined autoclave and placed at 100 °C for 24 h. The autoclave was cooled down in natural way; the precipitates were collected by filtration, washed five times with DD water and kept at 45 °C overnight for drying after centrifugation. Under same conditions, other control samples were also prepared as shown in table S1.

2.4. Anion interchange treatment

NiAl LDH with NO_3^- interlayer ions was synthesized by ion exchange treatment. Typically, 0.6 g of NiAl LDH-CO_3^{2-} was mixed thoroughly in 650 ml aqueous solution of 1.5 M $NaNO_3$ and 4 mM HNO_3 purged with N_2 and stirred mechanical on shaker for 24 h at ambient conditions. The as-prepared NiAl LDH-NO_3^- was washed many times with N_2 purged DD water and dried at 45 °C after centrifugation.

2.5. Delamination of NiAl LDH and GO precursors

The delamination of NiAl LDH nanosheets was completed by continuous mechanical stirring in formamide. Briefly, 100 mg NiAl LDH-NO_3^- was mixed homogeneously in 300 ml of formamide and placed on mechanical shaker at 120 rpm for 72 h. The supernatant was collected after centrifuging at 4000 rpm for 10 min.

To acquire exfoliated graphene oxide (GO) monolayers, firstly GO was prepared by modified Hummer method [28]. We used DMF as exfoliating agent instead of commonly employed water, and this is the significant point of our new strategy. Typically, 30 mg GO was thoroughly dispersed in 100 ml DMF by 8 h of vigorous sonication. The centrifugation at 12000

rpm was used to get supernatant and it was made diluted to 200 ml by adding formamide under continuous stirring.

2.6. Co-feeding protocol for NiAl LDH/GO LBL self-assembly

Controllable co-feeding protocol was designed to yield layer-by-layer self-assembly of NiAl LDH/GO LBL superlattice composite. In co-feeding process, two separate solutions containing 200 ml of each exfoliated NiAl LDH and GO supernatant were dropped at a well-controlled speed of 1.5 ml/min into another solution of 200 ml formamide under vigorous stirring. After completely adding up the two feed solution at controlled rate, the mixed solution was further stirred for 2 hours. The LBL superlattice nanocomposites were got recovered by centrifuging of product, repeated washing with ethanol and water and then freeze-dried. To achieve NiAl LDH/G with reduced graphene in above recovered product, 40 mg of as-prepared NiAl LDH/GO was placed in a small vessel and that was kept in another big vessel containing 600 µl of hydrazine (85%) to circumvent direct contact of two species. Finally, the air tight vessel was positioned at 90 °C for 12 h. Under same conditions, other control samples were also fabricated as shown in table S2.

2.7. Modification of electrode

To acquire the modified GCE, firstly the surface of GCE (3 mm diameter) was finely polished with 0.3 and 0.05 µm alumna slurry on microcloth pads and then rinsed with doubly distilled water. Subsequently, GCE was washed ultrasonically in DD water and ethanol and then allowed to dry under N_2 purging. A homogeneous mixture of 3 mg of NiAl LDH/G LBL composite in 1 ml of DD water was prepared under vigorous stirring. Secondly, 5 µl of above

suspension was casted on polished surface of GCE and dried under ambient temperature for further use. Finally the image of modified GCE is shown in scheme 1A.

2.8. Fabrication of electrochemical cell

The self-made electrochemical cell was designed and constructed. The photograph of as-constructed self-made electrochemical cell is depicted in scheme 1B. As can be seen that the cell is made of glass and covered with lid having four holes through which three electrodes are immersed into target analyte and fourth one is used for N_2 purging when necessary. The electrodes are fixed through positioning them in their respective holes as well as fixing the lid on the tope of cell. After purging N_2 for 15 min, 10 ml of PBS was poured into cell and CV measurements were conducted with NiAl LDH/G LBL/GCE in blank PBS between (-0.2 V to 0.6 V) by using CHI760 electrochemical workstation (CH Instrument Company, Shanghai, China). Then 50 µl of 0.1 M DA was injected in above solution and CV responses were recorded again in the presence of DA.

2.9. Choice of materials

The choice of materials always remains critically important for researchers to get superior catalytic activity. Among the transition metals, Ni has always enhanced electrocatalytic aptitude for oxidation reactions because of $Ni(OH)_2$/NiOOH redox process on electrode surface, low cost, good mechanical strength and electron transportation [29]. The boosted up catalytic reactivity of Ni centers is owing to the cases of filling *d* orbital. The Band theory explains the bonding that is derived by the interaction between positively charged ions and valence electrons. Accordingly, in transition metals the overlapping exists between *s* orbital and *d* orbital affecting the filling of *d* electrons. Instead of entering 10 electrons on *3d* band of Ni, only 8 could enter after completely

filling of *4s* due to the band overlapping of *4s* orbital and *3d* creating band holes. The presence of these band holes endow the metals with capability of accepting electrons from outside and absorbing species with band construction that consequently increase catalytic efficiency. [30] Here we preferred to use layer-by-layer assembly of exfoliated NiAl LDH and graphene layers rather than using direct mixing of two materials without exfoliation. It is because the insertion of highly conductive graphene layers between the interlayer galleries of LDH is possibly achieved by mixing exfoliated nanosheets of both materials with systematically controlled co-feeding protocol which in turn enhances electron shuttling. Therefore, it is expected that good catalytic activity of NiAl LDH and high conductivity of graphene synergistically would improve electrochemical sensing performance. The suggested pathways for possible catalytic mechanism would be predicted as follows;

$$Ni(OH)_2 + OH^- \longrightarrow NiOOH + H_2O + e^- \quad (1)$$

$$Ni^{3+} + \text{Dopamine} \longrightarrow Ni^{2+} + \text{Dopamine-o-quinone} \quad (2)$$

3. Results and discussion

3.1. Characterization of NiAl LDH/G LBL nanohybrid

Self-assembled superlattice system executing as positive and negative charged building blocks respectively, was achieved by successfully integrating NiAl LDH nanosheets with graphene monolayers as depicted by Fig. 1.

The morphologies of heterostacked composites were investigated by SEM at various magnifications. The SEM image of as-fabricated NiAl LDH/G in Fig. 2A shows typical platelet

like hexagonal flakes, demonstrating well restored LHD structure while re-stacking assembly of two oppositely charged nanosheets. Well-ordered layer-by-layer shaped morphology of resulting superlattice LDHs and graphene monolayers has been presented in Fig. 2B. This typical hexagonal structure of LDHs has been precisely retained after carefully executing the anion exchange process (Fig. S1). Furthermore, the clear evidences of well-organized structure of superlattice material were witnessed by TEM image in Fig. 2C. The high resolution TEM (HRTEM) image in Fig. 2D displays that every period of lamellar fringes has alternate layers with *d*-spacing of 0.92 nm which consequently authenticates successful insertion of graphene layers into NiAl LDH nanosheets, and also negates the possibility of anions/solvent insertion in between the interlayer gallery.

The SEM-EDX mapping results in Fig. 2E indicate a uniform distribution of Ni, Al, C and O elements respectively. The aforementioned results substantially authenticate the true heterostacked assembly of NiAl LDH/G superlattice.

The FTIR spectrum shows the successful incorporation of CO_3^{-2}, NO_3^- and G species between the interlayer regions as shown in Fig. 3A. The very broad absorption at 3457 cm^{-1} belongs to stretching vibration of H_2O and hydrogen bonded –OH groups present in samples. The shifting of strong absorption band from 1354 cm^{-1} analogous to CO_3^{-2} to another intense absorption band at 1387 cm^{-1} corresponding to NO_3^- is owing to the result of efficient ion interchange treatment. A very small absorption peak at 1630 cm^{-1} is may be due to C=C vibrations resulting from graphitic domains of graphene and bending vibration of H_2O [31]. The absorption peak at 1104 cm^{-1} designated to reduced graphene oxide which is an agreeable segregation between pure LDHs and composite LDH-G materials.[32].

Fig. 3B shows the typical XRD pattern of NiAl LDH/G LBL nanohybrid material with interlayer gallery spacing of 0.93 nm. This *d*-spacing value is almost similar with the sum-up thickness values of NiAl LDH monolayer (0.49 nm) and graphene nanosheet (0.41 nm), further it is also comparable with 0.92 nm HRTEM fringe spacing of two alternative layers of same heterostacked hybrid material. It is noteworthy that the appearance of crystallographic peak of (002) around 21° with interlayers spacing of 0.54 nm undoubtedly authenticates the construction of layer-by-layer self-assembly of NiAl LDH/G hybrid material. The enlargement in basal spacing of NiAl LDH material from 0.73 nm to 0.84 nm is due to the effective replacement of CO_3^{-2} with larged size NO_3^- species by efficient ion exchange treatment [33] (Fig. S2). Additionally, A couple of in-plane basal peaks (100) and (110) originated at 34° and 61° approve the LDH existence in superlattice as well as confirm the maintained 2D structure of LBL hybrid material. In comparison, without following co-feeding protocol, most of the LDH nanolayers are re-stacked with each other forming no LBL material when NiAl LDH solution is directly poured in graphene solution (Fig. S3).

For further investigations, XPS measurements were executed in order to evaluate the valence oxidation states of elements present in NiAl LDH/G LBL material. The wide scan spectrum of NiAl LDH/G LBL hybrid nanoarchitectures illustrates that the material is composed of Ni, O, C and Al as shown in Fig. 3C. The core fitting spectrum of Ni has been displayed in Fig. 3D, which is further splitted into two peaks Ni 2p3/2 and Ni 2p1/2 centered at 856.4 eV and 874.1 eV having two satellite peaks and with spin energy gap of 17.7 eV, which approve the existence of Ni^{+2} species in LDH/G based LBL nano hybrid [34].

3.2. Electrochemical performance of NiAl LDH/G hydride electrode.

The interfacial charge transfer characteristics of bare electrode, modified with NiAl LDH and NiAl LDH/G LBL nanohybrids were investigated by performing electrochemical impedance spectroscopy (EIS) in $[Fe(CN)_6]^{3-/4}$ redox solution as presented in Fig. 4A. Inset is the Randle equivalence circuit diagram which is fitted with solution resistance (*Rs*), charge transfer resistance (*Rct*), double layer capacitance (*Cdl*), and Warburg constant (*W*), respectively. Compared with *Rct* value of 431 Ω shown by NiAl LDH/G LBL electrode, NiAl LDH exhibited a very large *Rct* value of 1967 Ω which is because of semiconductive nature of LDH materials. The very low electron transferring resistance demonstrated by our heterostacked LBL assembled NiAl LDH/G electrode is due to the fact that reduced graphene nanosheets inserted in interlayer spaces of LDHs enrich numerous small energy gaps, which are responsible for interfacial charge transfer aptitude [35]. Similar results have also been achieved by recording CV curve different modified electrodes in $[Fe(CN)_6]^{3-/4}$ redox solution (Fig. S4). The electrochemical active surface areas of the electrodes are calculated according the Randles–Sevcik equation. [36-38]

$$Ip = (2.69 \times 10^5)n^{3/2}AC^*D^{1/2}v^{1/2} \qquad (3)$$

The estimated electrochemical active surface area of NiAl LDH/G LBL/GCE (0.112 cm^2) is higher than NiAl LDH /GCE (0.094 cm^2) and bare GCE (0.073 cm^2) respectively. The boosted up electroactive surface area of NiAl LDH/G LBL modified electrode confirms the synergy effect of NiAl LDH and graphene to provide an effective platform and large surface in facilitating electron transportation between electrode and target solution.

To measure electrocatalytic abilities of NiAl LDH/G modified electrode, cyclic voltammetry (CV) was executed in the absence and presence of 0.5 mM DA in 0.1 M PBS (pH 7.4) as presented in Fig. 4B. The distinct redox peaks are recorded in the presence of 0.5 mM DA corresponding to the oxidation of DA to equinone and consequently the reduction of equinone to

DA [39, 40]. The differential pulse voltammetry (DPV) curves have also been recorded with varied concentrations of DA in 0.1 M PBS (pH 7.4) as depicted by Fig. S5. By augmenting DA concentration, the oxidation peak current density is also going to increase linearly. To compare the results of NiAl LDH/G LBL nanohybrid in DA detection, we have also explored the electrocatalytic activities of as-fabricated other nanocatalysts such as graphene, NiAl LDH, and NiAl LDH/G (direct mixing) under same conditions as demonstrated by Fig. 4C. In comparison to graphene and NiAl LDH electrodes, NiAl LDH/G direct mixing illustrates higher oxidation peak current but lower than NiAl LDH/G LBL electrode. This is owing to the fact of good conductivity of graphene coupled with NiAl LDH direct mixing nanocomposites. The superb electrocatalytic properties presented by NiAl LDH/G LBL nanohybrids may be because of different aspects: (i) the inclusion of π-electron-rich nanosheets of extremely conductive graphene substrate between the interlayer spaces of NiAl LDHs to assist quick electron transport; (ii) the LBL nanohybrid material holds high surface area; (iii) the rapid accessibility of DA molecules to rough surface of heterostacked LBL nanohybrid material; (iv) the structural integration of charged nanosheets creates slight modification in electronic structure of NiAl LDH/G LBL nanohybrids at nanoscale interface [26, 41]. Fig. S6 (A) and (B) show the CV curves of GCE's modified by different NiAl LDH materials with varied Ni contents and NiAl LDH/G LBL with varied amount of graphene inserted in between NiAl LDH layers. The admirable sensing capabilities of NiAl LDH/G LBL electrode endorse enlarged surface area providing more active sites, synergistic effect between NiAl LHDs and graphene, unique well-ordered LBL morphology which contributes to maximum interfacial effect between LDHs and graphene layers.

Probably, there are two potential biomolecules AA and UA that can cause interferences while detecting DA from biological fluids. We confirm the DA measurement in the presence of AA and UA as shown by the Fig. 4D. The oxidation peak current signal of DA 50 µM alone is almost the same when different concentrations of AA 10 µM and UA 10 µM first separately and then together (AA10 µM + UA 10 µM) are added in the same concentration of DA. It is worth mentioning that the electrode modified by NiAl LDH/G LBL which possesses various interfacial collaborations within LBL nanocomposites has been employed with structurally different biotic molecules, which assured the probability to separately detect DA from mixed solution of AA and UA. Moreover, amperometric measurements were performed to test the sensitivity of NiAl LDH/G LBL biosensor upon the successive addition of various concentrations of DA in stirring PBS at an applied potential of 0.14 V (Fig. 5A). A quick response is detected by adding 0.1 µM to 97 µM DA, which attains the steady-state current condition of ~95% within 3 s. The rapid response to DA additions may be due to the fact of prompt accessibility of DA molecules to rough surface, enhanced surface active sites and instant electron transport kinetics of heterostacked LBL nanohybrids. The broad linear range and low detection limit of 2 nM signal-to-noise factor of 3 (S/N=3) has been achieved by our proposed biosensor and these reports are even superior than most of electrochemical performances in DA detection compared with recent data from literature as presented by Table S3. Fig. 5B shows the linear range of oxidation peak current *versus* DA concentrations R^2 value of 0.995.

The selectivity of biosensor was further examined in the presence of certain interfering species such as AA, UA, H_2O_2, glucose, KCl and NaCl that commonly may co-exist in blood and it is crucially important to measure the effect of these species [42, 43]. To improve the selectivity of NiAl LDH/G LBL nanohybrids towards DA, the NiAl LDH/G LBL electrode was modified with 5 µL of varied percentage of biocompatible polymer Nafion (0.25%, 0.5% and 0.75%)

which has already been used to modify electrodes in biosensors. The 5 µL of 0.75% Nafion modified electrode gave the best anti-interference capability to AA and DA. In PBS solution (pH=7.4), Nafion is negatively charged that could efficiently reduce the interference from other negatively charged biomolecules such as UA and AA by electrostatic interaction [44, 45]. The modified surface of electrode can easily attract positively charged aromatic DA molecules through π–π stacking and electrostatic attraction while repelling electronegative AA and UA molecules and consequently the selectivity is improved. The clear current signals are observed upon the addition of successive amount of DA but there is no obvious signal upon the inoculation of 80-folds higher concentrations as DA for each of interfering substances (0.8 mM of UA, AA and glucose) in stirring 0.1 M PBS at an applied potential of 0.14 V as demonstrated by Fig. 5C. Moreover, no interference could be observed upon 1 mM addition of all other potential interfering metal ions during DA detection. The concentration of 0.8 mM of UA and AA could not create any noticeable interference even these concentrations are much higher than physiological ranges. The high selectivity and sensitivity may be accredited to the high electron density of NiAl LDH/G LBL and sulfonic groups of Nafion. In anti-interference assay, we have used Nafion film as modifier of NiAl LDH/G LBL electrode to inhibit the interference of biologically co-existive molecules. Therefore, we have performed some additional experiments to evaluate the sensitivity of NiAl LDH/G LBL electrode after modification with Nafion film. As presented by Fig. S7, the oxidation current densities of NiAl LDH/G LBL electrodes modified with Nafion (red line) and without modified (black line) to the addition of different concentrations of DA are almost same ensuring the good sensitivity of NiAl LDH/G LBL electrode after modification with Nafion film. Fouling is one of the common issues that ever encounters during electrochemical detection of dopamine and causes the sensor performance degradation [46]. There exists fouling to some extent because in biological conditions the surface of electrode may undoubtedly be blocked by the biomolecules present in the sample which in turn jeopardize the long term stability of electrode. There are two types of fouling which can be described: (i) passive biological fouling due to background species of proteins or lipids which adhere to electrode surface, whether it is active or not, and (ii) electrochemical fouling where an insulating film is formed on electrode surface because of the reactions occur for detection of analyte and this is typical of the oxidation of DA. During electrochemical oxidation, DA is converted into dopaminoquinone *via* two-electron transfer then this intermediate undergoes

protonation of amine leading to leucodopaminochrome which further undergoes two-electron transfer giving dopaminochrome. Finally, through free radical polymerization, dopaminochrome may polymerize to melanin on electrode that can considerably hinder the surface dependent redox properties of DA [47]. In Fig. S8, the oxidation current density is going to decrease slightly with time in the presence of 200 µM DA owing to the adsorption of some oxidation products of DA on active cites of material. In contrast, oxidation current density of 10 µM DA is almost same with time. While investigating long-term stability, the electrode modified by NiAl LDH/G LBL material exhibited a retained response value of 90.8% compared with its initial peak current value to oxidation of 0.5 mM DA up to 25 days of post modification (Fig. 5D). To ensure reproducibility of biosensor, six electrodes were modified with NiAl LDH/G LBL material and recorded their current response values in the presence of 0.5 mM DA showing relative standard deviation (RSD) value less than 5%. The four successive assays of same electrode present the reproducible current with RSD less than 5% (Fig. 5D inset). The decline in sensitivity is due to fouling of electrode surface. The aforementioned results validate decent stability and reproducibility of self-made biosensing platform.

3.3. Real-time in-vitro detection of DA from live cells

Intractable psychiatric and chronic neurodegenerative disorders such as Parkinson's diseases (PD) have seriously threatened the public health worldwide because many of dopaminergic neurons present in substantia nigra of PD patients are destroyed before it is being clinically diagnosed. The second high mortality neurodegenerative disease PD gradually promotes the loss of movement, balance and muscle control [48, 49]. The early diagnosis of these lethal syndromes is the one and only way to upsurge the survival rate and get rid of them. Once enhanced sensitivity successfully achieved, the practical application of as-fabricated NiAl LDH/G LBL based biosensor has been assessed in real-time detection of DA secretions from human neuronal functioning neuroblastoma cell line (SH-SY 5Y) after being motivated by the addition highly K^+ buffer solution.

Fig. 6A presents the bright field image of live neuronal neuroblastoma cell line (SH-SY 5Y). Furthermore, the CCK-8 assay has been used to evaluate the biocompatibility of as-prepared material to living cells, which shows that cells maintain 98.1%, 96.9%, 92.7%, 90.1% and 88.7% viability upon incubation with NiAl LDH/G LBL modified electrode for 1 h, 2 h, 3 h, 4 h and 5 h, respectively (Fig. 6B). As highly concentrated extracellular K^+ solution is added, depolarization of cell membrane occurs that produces an influx of Na^+ and Ca^{2+} channels [50]. As a result, the enhanced Ca^{2+} influx arouses many protein immobilization, diffusion of dense vehicle of cells and the level of voltage-sensitive Ca^{2+} species increases sufficiently to initiate exocytosis, consequently DA flux merged with cell membrane is evolved to extracellular region where it can be measured [51, 52]. The extracellular DA is measured by recording amperometric current signals to the oxidation of DA secretions after being triggered upon the inoculation of different spikes of K^+ solution in the absence and presence of (SH-SY 5Y) cell line and attained plateau value within 10 s as depicted by Fig. 6C. Undoubtedly, it is observed by adding every single spike of K^+ solution as stimulus that no current response has been measured in the absence of living cells while in the presence of cells, enhanced oxidation current signals are observed. The current responses for each and every spike are went on lessening subsequently generating oxidation current densities 2.12 $\mu A/cm^2$ 1.03 $\mu A/cm^2$ and 0.86 $\mu A/cm^2$ respectively (Fig. 6D). By using regression equation, quantity of endogenous DA concentration has been measured after being stimulated and found to be 0.21 μM, 0.13 μM and 0.11 μM respectively. Additionally, the DA concentrations in live cells have also been determined by conventional colorimetric method for comparison as shown in **Table 1**. The above stated results unequivocally authenticate the trustworthy presentation of NiAl LDH/G LBL nanohybrid material for real-time detection of DA secretions from live cells as Parkinson's diseases (PD) diagnostic probe.

412 **Table 1** Analytical performance of electrochemical method compared with standard colorimetric
413 method for detection of DA from live cells.

Spikes	Electrochemical method (μM)	Calorimetric method (μM)	Relative standard deviation (%)
1st	0.21	0.22	3.2
2nd	0.13	0.15	5.1
3rd	0.11	0.10	6.6

414

415 **4. Conclusion**

416 In conclusion, we have developed an alternately stacked heteroassembly of NiAl LDH/G
417 LBL on molecular-level by electrostatic interactions between oppositely charged nanosheets of
418 conductive graphene and catalytically active LDH. To overcome the problem of high insulating
419 nature of metal oxides/hydroxides, charge conducting graphene layers have been inserted in
420 between interlayer regions of LDH material which slightly modulates electronic structure at
421 nanoscale interface. In addition, the bottlenecks of enzyme based electrochemical sensors, such
422 as high cost and feeble stability of enzyme, and short storage and usage life-time of sensor have
423 also been overwhelmed by using as-prepared enzyme-less nanomaterial. Our electrochemical
424 biosensor based on NiAl LDH/G LBL nanohybrid has outperformed in quantitative detection of
425 DA under biological environment. Compared with numerous other reported DA biosensors, NiAl
426 LDH/G LBL modified electrode demonstrated excellent selectivity, durability, wide linear range
427 from 0.1 to 97 μM, and low detection limit reaching down to 2 nM. Moreover, the practical
428 application of this electrochemical biosensor has been explored in real-time *in-vitro* detection of

DA concentrations from live human nerve cell after being stimulated. Thus, our findings hold intriguing features of well-controlled, economical, high-yield process for self-assembled periodic stacking of 2D charged nanosheets, and open new horizon in exploring vertically stacked artificial 2D nanomaterials as-well-as inspiring application potential in biosensing podium, state-of-the-art biomedical devices and pathological diagnostics.

ASSOCIATED CONTENT

Supporting information available: Additional details, figures and tables as mentioned in the text. This material is available free of charge via the Internet.

Corresponding authors

*E-mail: liuhf@mail.hust.edu.cn

Notes

The authors declare no competing financial interest.

Acknowledgments

National Natural Science Foundation of China National Natural Science Foundation of China (No. 51572094), the Innovation Foundation of Huazhong University of Science (No. 2015TS150, 2015ZZGH010) and Technology and the Key Laboratory for Large-Format Battery Materials and System, ministry of Education and Fundamental Research Funds for the Central Universities (No. 2014QN110), We acknowledge the support of the Analytical and Testing Center of the Huazhong University of Science and Technology for SEM and XPS measurements.

References

[1] C. Yang, B. Gu, D. Zhang, C. Ge, H. Tao, Coaxial carbon fiber/ZnO nanorods as electrodes for the electrochemical determination of dopamine, Anal. Meth. 8 (2016) 650-655.

[2] Y. Li, H. Li, M. Li, C. Li, D. Sun, B. Yang, Porous boron-doped diamond electrode for detection of dopamine and pyridoxine in human serum, Electrochim. Acta, 258 (2017) 744-753.

[3] X. Zan, H. Bai, C. Wang, F. Zhao, H. Duan, Graphene paper decorated with a 2D array of dendritic platinum nanoparticles for ultrasensitive electrochemical detection of dopamine secreted by live cells, Chemistry, 22 (2016) 5204-5210.

[4] T.A. Mir, M.H. Akhtar, N.G. Gurudatt, J.I. Kim, C.S. Choi, Y.B. Shim, An amperometric nanobiosensor for the selective detection of K(+)-induced dopamine released from living cells, Biosen. Bioelectron. 68 (2015) 421-428.

[5] V.V. Sharma, I. Gualandi, Y. Vlamidis, D. Tonelli, Electrochemical behavior of reduced graphene oxide and multi-walled carbon nanotubes composites for catechol and dopamine oxidation, Electrochim. Acta, 246 (2017) 415-423.

[6] R. Cui, Y.P. Gu, L. Bao, J.Y. Zhao, B.P. Qi, Z.L. Zhang, Z.X. Xie, D.W. Pang, Near-infrared electrogenerated chemiluminescence of ultrasmall Ag2Se quantum dots for the detection of dopamine, Anal. Chem. 84 (2012) 8932-8935.

[7] E. Farjami, R. Campos, J.S. Nielsen, K.V. Gothelf, J. Kjems, E.E. Ferapontova, RNA aptamer-based electrochemical biosensor for selective and label-free analysis of dopamine, Anal. Chem. 85 (2013) 121-128.

[8] M. Asif, H. Liu, A. Aziz, H. Wang, Z. Wang, M. Ajmal, F. Xiao, Core-shell iron oxide-layered double hydroxide: High electrochemical sensing performance of H2O2 biomarker in live cancer cells with plasma therapeutics, Biosen. Bioelectron. 97 (2017) 352-359.

[9] P. Hashemi, H. Bagheri, A. Afkhami, Y.H. Ardakani, T. Madrakian, Fabrication of a novel aptasensor based on three-dimensional reduced graphene oxide/polyaniline/gold nanoparticle composite as a novel platform for high sensitive and specific cocaine detection, Anal. Chim. Acta, 996 (2017) 10-19.

[10] G. Yang, F. Zhao, B. Zeng, Electrochemical determination of cefotaxime based on a three-dimensional molecularly imprinted film sensor, Biosen. Bioelectron. 53 (2014) 447-452.

[11] H. Bagheri, N. Pajooheshpour, B. Jamali, S. Amidi, A. Hajian, H. Khoshsafar, A novel electrochemical platform for sensitive and simultaneous determination of dopamine, uric acid

and ascorbic acid based on Fe3O4SnO2Gr ternary nanocomposite, Microchem. J. 131 (2017) 120-129.

[12] X. Zhang, Y.C. Zhang, L.X. Ma, One-pot facile fabrication of graphene-zinc oxide composite and its enhanced sensitivity for simultaneous electrochemical detection of ascorbic acid, dopamine and uric acid, Sens. Actua. B: Chemical, 227 (2016) 488-496.

[13] W. He, Y. Ding, L. Ji, X. Zhang, F. Yang, A high performance sensor based on bimetallic NiCu nanoparticles for the simultaneous determination of five species of biomolecules, Sens. Actua. B: Chemical, 241 (2017) 949-956.

[14] H. Bagheri, A. Afkhami, P. Hashemi, M. Ghanei, Simultaneous and sensitive determination of melatonin and dopamine with Fe3O4 nanoparticle-decorated reduced graphene oxide modified electrode, RSC Advances, 5 (2015) 21659-21669.

[15] S. Pruneanu, A.R. Biris, F. Pogacean, C. Socaci, M. Coros, M.C. Rosu, F. Watanabe, A.S. Biris, The influence of uric and ascorbic acid on the electrochemical detection of dopamine using graphene-modified electrodes, Electrochim. Acta, 154 (2015) 197-204.

[16] Z. Xu, L. Yang, C. Xu, Pt@UiO-66 heterostructures for highly selective detection of hydrogen peroxide with an extended linear range, Anal. Chem. 87 (2015) 3438-3444.

[17] M. Yuan, A. Liu, M. Zhao, W. Dong, T. Zhao, J. Wang, W. Tang, Bimetallic PdCu nanoparticle decorated three-dimensional graphene hydrogel for non-enzymatic amperometric glucose sensor, Sens. Actua. B: Chemical, 190 (2014) 707-714.

[18] M. Asif, W. Haitao, D. Shuang, A. Aziz, G. Zhang, F. Xiao, H. Liu, Metal oxide intercalated layered double hydroxide nanosphere: With enhanced electrocatalyic activity towards H2O2 for biological applications, Sens. Actua. B: Chemical, 239 (2017) 243-252.

[19] Z.P. Xu, J. Zhang, M.O. Adebajo, H. Zhang, C. Zhou, Catalytic applications of layered double hydroxides and derivatives, Appl. Clay Sci., 53 (2011) 139-150.

[20] A.I. Khan, D. O'Hare, Intercalation chemistry of layered double hydroxides: recent developments and applications, J. Mater. Chem. 12 (2002) 3191-3198.

[21] L. Chen, K. Sun, P. Li, X. Fan, J. Sun, S. Ai, DNA-enhanced peroxidase-like activity of layered double hydroxide nanosheets and applications in H2O2 and glucose sensing, Nanoscale, 5 (2013) 10982-10988.

[22] Q. Wang, D. O'Hare, Recent advances in the synthesis and application of layered double hydroxide (LDH) nanosheets, Chemical Rev.112 (2012) 4124-4155.

[23] R. Ma, T. Sasaki, Nanosheets of oxides and hydroxides: Ultimate 2D charge-bearing functional crystallites, Adv. Mater. 22 (2010) 5082-5104.

[24] M.Q. Zhao, Q. Zhang, J.Q. Huang, F. Wei, Hierarchical nanocomposites derived from nanocarbons and layered double hydroxides-properties, synthesis, and applications, Adv. Funct. Mater. 22 (2012) 675-694.

[25] R. Ma, X. Liu, J. Liang, Y. Bando, T. Sasaki, Molecular-scale heteroassembly of redoxable hydroxide nanosheets and conductive graphene into superlattice composites for high-performance supercapacitors, Adv. Mater. 26 (2014) 4173-4178.

[26] W. Ma, R. Ma, C. Wang, J. Liang, X. Liu, K. Zhou, T. Sasaki, A superlattice of alternately stacked Ni–Fe hydroxide nanosheets and graphene for efficient splitting of water, ACS Nano, 9 (2015) 1977-1984.

[27] M. Asif, A. Aziz, A.Q. Dao, A. Hakeem, H. Wang, S. Dong, G. Zhang, F. Xiao, H. Liu, Real-time tracking of hydrogen peroxide secreted by live cells using MnO2 nanoparticles intercalated layered doubled hydroxide nanohybrids, Anal. Chim. Acta, 898 (2015) 34-41.

[28] D.C. Marcano, D.V. Kosynkin, J.M. Berlin, A. Sinitskii, Z. Sun, A. Slesarev, L.B. Alemany, W. Lu, J.M. Tour, Improved synthesis of graphene oxide, ACS Nano, 4 (2010) 4806-4814.

[29] R.K. Shervedani, M. Karevan, A. Amini, Prickly nickel nanowires grown on Cu substrate as a supersensitive enzyme-free electrochemical glucose sensor, Sens. Actua. B: Chemical, 204 (2014) 783-790.

[30] W. He, Y. Ding, W. Zhang, L. Ji, X. Zhang, F. Yang, A highly sensitive sensor for simultaneous determination of ascorbic acid, dopamine and uric acid based on ultra-small Ni nanoparticles, J. Electroanal. Chem. 775 (2016) 205-211.

[31] L. Zhang, J. Wang, J. Zhu, X. Zhang, K. San Hui, K.N. Hui, 3D porous layered double hydroxides grown on graphene as advanced electrochemical pseudocapacitor materials, J. Mater. Chem. A, 1 (2013) 9046.

[32] M. Li, J.P. Cheng, J. Wang, F. Liu, X.B. Zhang, The growth of nickel-manganese and cobalt-manganese layered double hydroxides on reduced graphene oxide for supercapacitor, Electrochim. Acta, 206 (2016) 108-115.

[33] L. Ma, Q. Wang, S.M. Islam, Y. Liu, S. Ma, M.G. Kanatzidis, Highly selective and efficient removal of heavy metals by layered double hydroxide intercalated with the MoS4(2-) ion, J. Am. Chem. Soci.138 (2016) 2858-2866.

[34] M. Li, F. Liu, J.P. Cheng, J. Ying, X.B. Zhang, Enhanced performance of nickel–aluminum layered double hydroxide nanosheets/carbon nanotubes composite for supercapacitor and asymmetric capacitor, J. All. Comp. 635 (2015) 225-232.

[35] K. Ghanbari, M. Moloudi, Flower-like ZnO decorated polyaniline/reduced graphene oxide nanocomposites for simultaneous determination of dopamine and uric acid, Anal. Biochem. 512 (2016) 91-102.

[36] T. Rahmani, A. Hajian, A. Afkhami, H. Bagheri, A novel and high performance enzyme-less sensing layer for electrochemical detection of methyl parathion based on BSA templated Au-Ag bimetallic nanoclusters, New J. Chem. 42 (2018) 7213-7222.

[37] H. Bagheri, A. Afkhami, H. Khoshsafar, A. Hajian, A. Shahriyari, Protein capped Cu nanoclusters-SWCNT nanocomposite as a novel candidate of high performance platform for organophosphates enzymeless biosensor, Biosen. Bioelectron. 89 (2017) 829-836.

[38] A.J. Ghazizadeh, A. Afkhami, H. Bagheri, Voltammetric determination of 4-nitrophenol using a glassy carbon electrode modified with a gold-ZnO-SiO2 nanostructure, Mikrochim. Acta, 185 (2018) 296.

[39] B. Li, Y. Zhou, W. Wu, M. Liu, S. Mei, Y. Zhou, T. Jing, Highly selective and sensitive determination of dopamine by the novel molecularly imprinted poly (nicotinamide)/CuO nanoparticles modified electrode, Biosen. Bioelectron. 67 (2015) 121-128.

[40] Y.J. Yang, W. Li, CTAB functionalized graphene oxide/multiwalled carbon nanotube composite modified electrode for the simultaneous determination of ascorbic acid, dopamine, uric acid and nitrite, Biosen. Bioelectron. 56 (2014) 300-306.

[41] X. Long, J. Li, S. Xiao, K. Yan, Z. Wang, H. Chen, S. Yang, A strongly coupled graphene and FeNi double hydroxide hybrid as an excellent electrocatalyst for the oxygen evolution reaction, Angew. Chem. Int. Ed. 53 (2014) 7584-7588.

[42] J. Salamon, Y. Sathishkumar, K. Ramachandran, Y.S. Lee, D.J. Yoo, A.R. Kim, One-pot synthesis of magnetite nanorods/graphene composites and its catalytic activity toward electrochemical detection of dopamine, Biosen. Bioelectron. 64 (2015) 269-276.

[43] Y. Ma, M. Zhao, B. Cai, W. Wang, Z. Ye, J. Huang, 3D graphene foams decorated by CuO nanoflowers for ultrasensitive ascorbic acid detection, Biosen. Bioelectron. 59 (2014) 384-388.

574 [44] H.S. Wang, T.H. Li, W.L. Jia, H.Y. Xu, Highly selective and sensitive determination of
575 dopamine using a Nafion/carbon nanotubes coated poly(3-methylthiophene) modified electrode,
576 Biosen. Bioelectron. 22 (2006) 664-669.
577 [45] M. Zhang, C. Liao, Y. Yao, Z. Liu, F. Gong, F. Yan, High-performance dopamine sensors
578 based on whole-graphene solution-gated transistors, Adv. Funct. Mater. 24 (2014) 978-985.
579 [46] Q. Yuan, Y. Liu, C. Ye, H. Sun, D. Dai, Q. Wei, G. Lai, T. Wu, A. Yu, L. Fu, K.W.A. Chee,
580 C.T. Lin, Highly stable and regenerative graphene-diamond hybrid electrochemical biosensor for
581 fouling target dopamine detection, Biosen. Bioelectron. 111 (2018) 117-123.
582 [47] W. Harreither, R. Trouillon, P. Poulin, W. Neri, A.G. Ewing, G. Safina, Carbon nanotube
583 fiber microelectrodes show a higher resistance to dopamine fouling, Anal. Chem. 85 (2013)
584 7447-7453.
585 [48] T. Bryan, X. Luo, L. Forsgren, L.A. Morozova-Roche, J.J. Davis, The robust
586 electrochemical detection of a Parkinson's disease marker in whole blood sera, Chem. Sci. 3
587 (2012) 3468-3473.
588 [49] B.R. Haas, T.H. Stewart, J. Zhang, Premotor biomarkers for Parkinson's disease-a
589 promising direction of research, Transl. Neurodegen. 1 (2012) 11.
590 [50] H.G. Sudibya, J. Ma, X. Dong, S. Ng, L.J. Li, X.W. Liu, P. Chen, Interfacing glycosylated
591 carbon-nanotube-network devices with living cells to detect dynamic secretion of biomolecules,
592 Ange. Chem. Int. Ed. 48 (2009) 2723-2726.
593 [51] S. Hou, M.L. Kasner, S. Su, K. Patel, R. Cuellari, Highly sensitive and selective dopamine
594 biosensor fabricated with silanized graphene, J Phy Chem C, 114 (2010) 14915-14921.
595 [52] B.R. Li, Y.J. Hsieh, Y.X. Chen, Y.T. Chung, C.Y. Pan, Y.T. Chen, An ultrasensitive
596 nanowire-transistor biosensor for detecting dopamine release from living PC12 cells under
597 hypoxic stimulation, J. Am. Chem. Soci. 135 (2013) 16034-16037.

598

599

600

601

602 **Figures and captions**

603

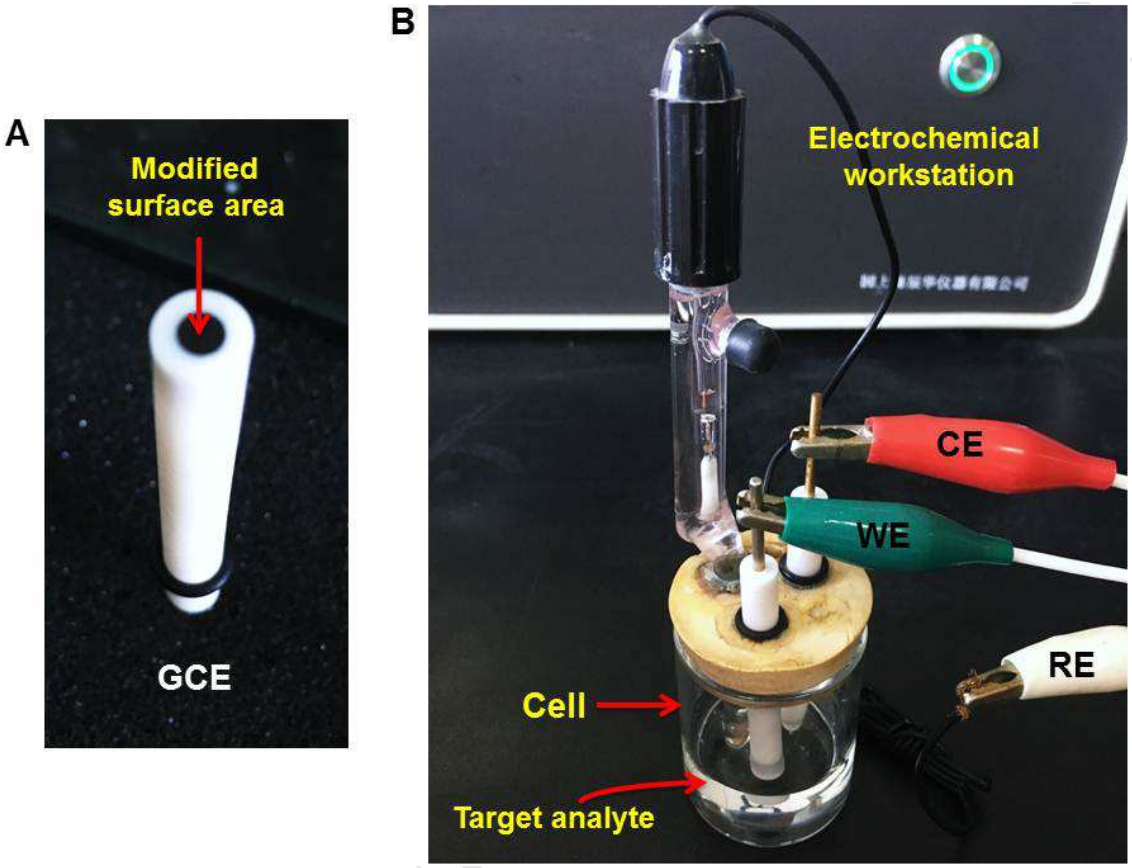

604

605 **Scheme 1.** The photographs of (A) GCE with modified surface, (B) self-made electrochemical

606 cell

607

608

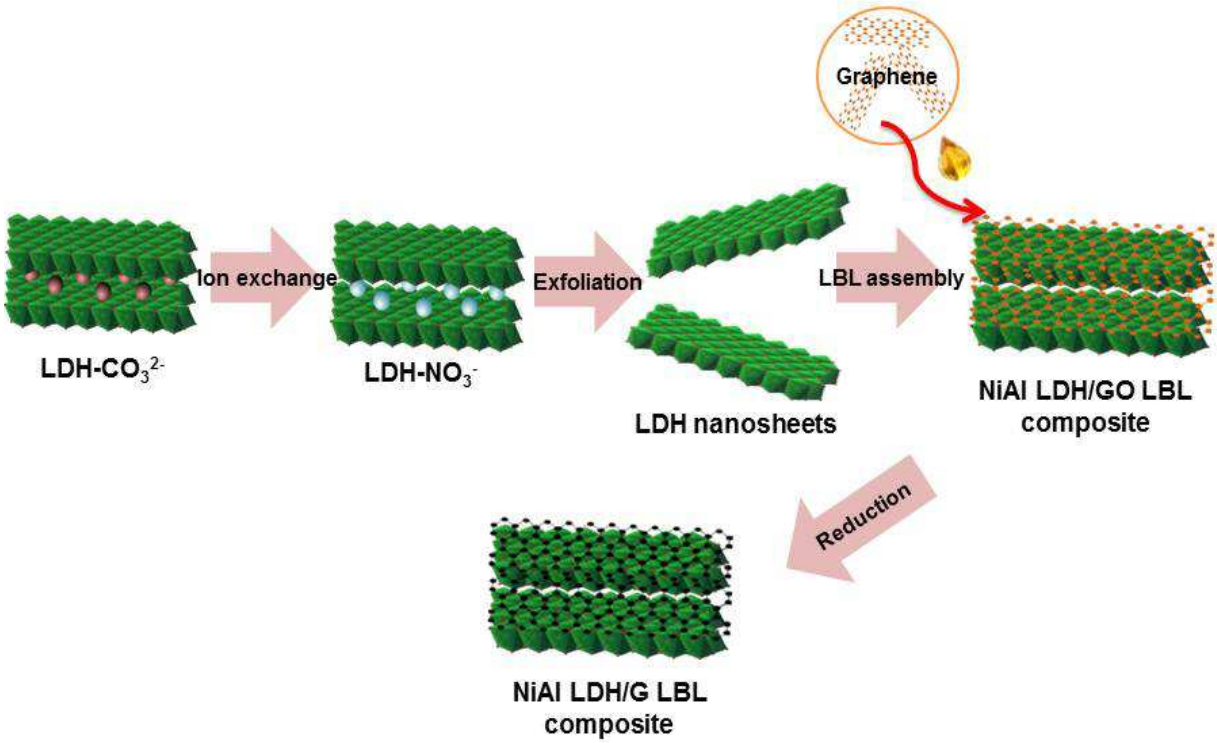

609 **Fig. 1.** Flow chart presentation of different steps involved in the fabrication mechanism of NiAl

610 LDH/G LBL nanocomposites.

611

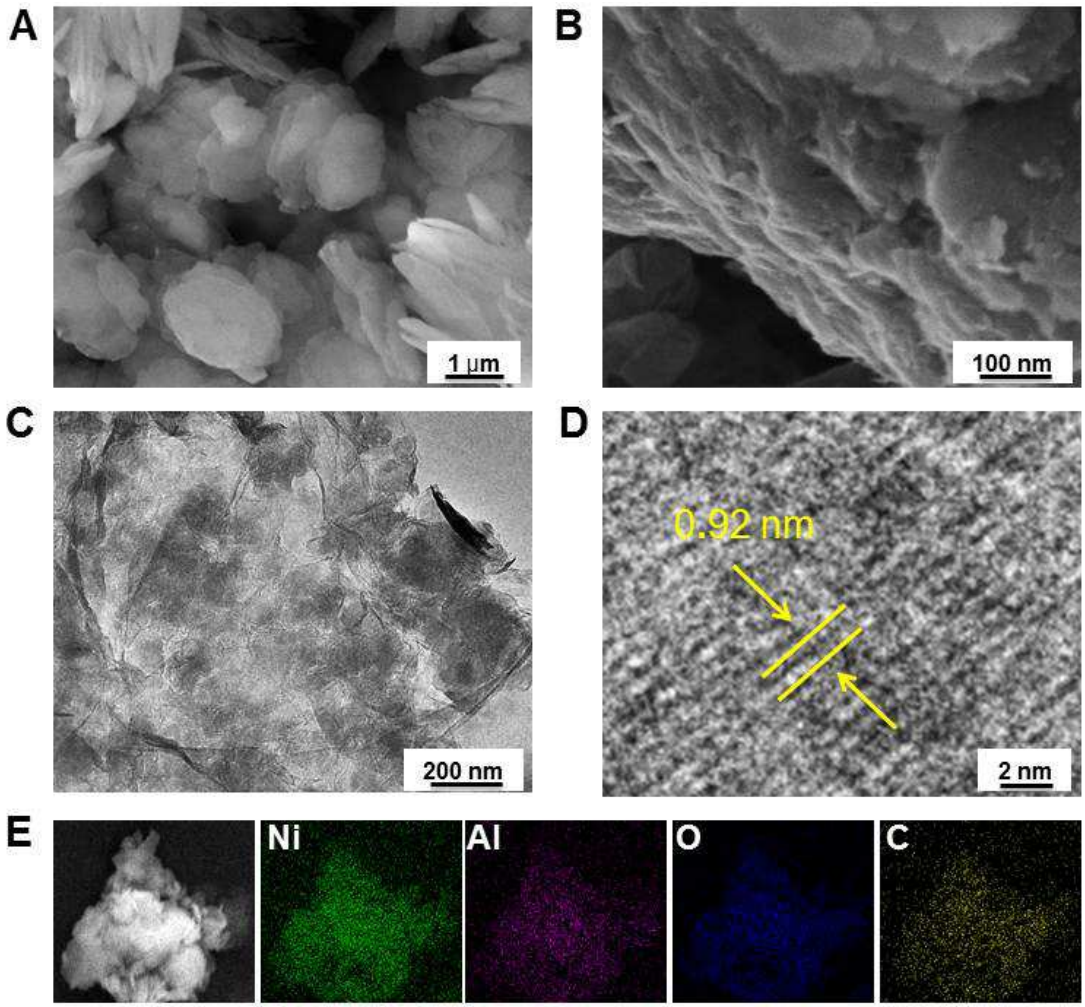

612

613 **Fig. 2.** Morphological analysis of LBL-assembled product, (A and B) SEM, (C) TEM images at
614 various magnifications and (D) HRTEM image, and (E) SEM-EDX mapping results of NiAl
615 LDH/G LBL nanocomposites.

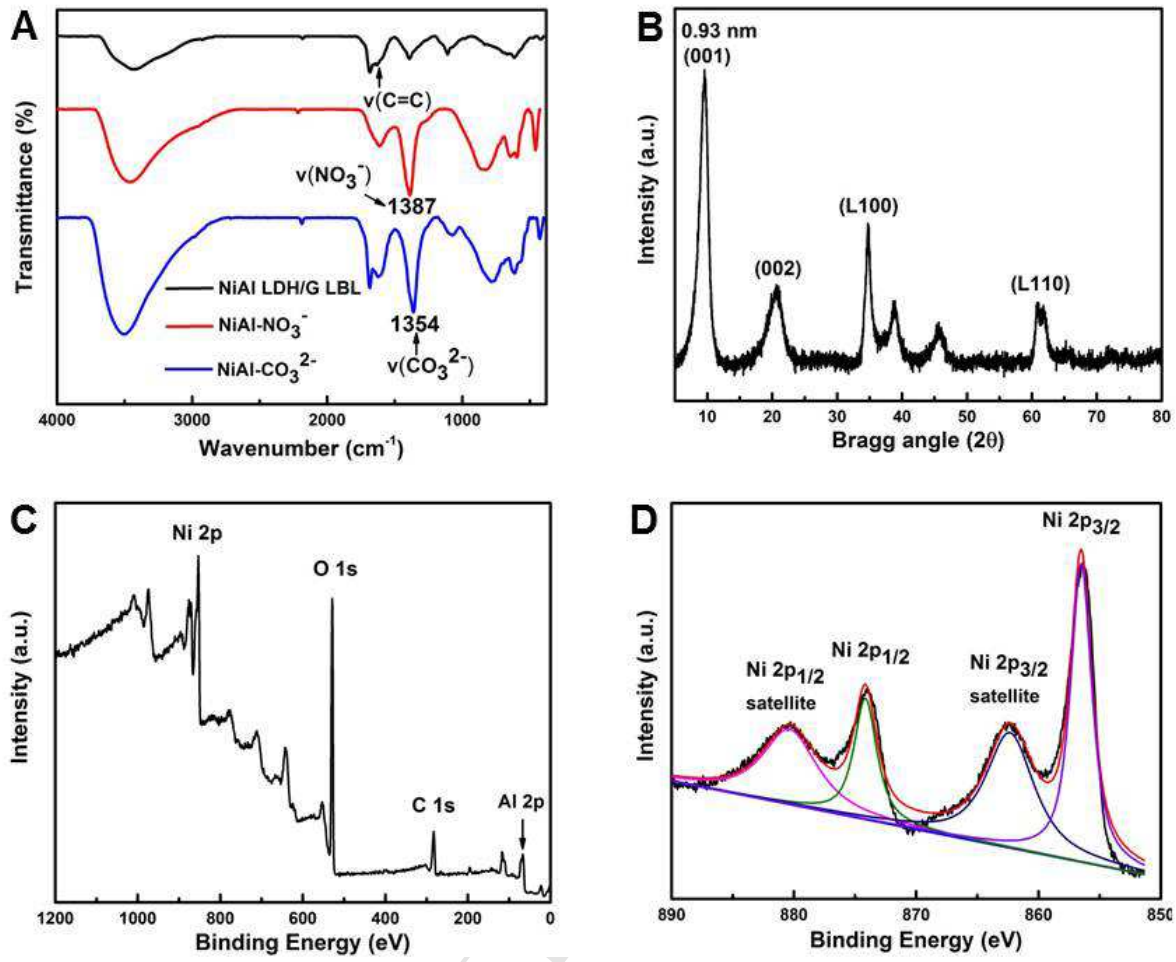

Fig. 3. (A) FTIR spectra of NiAl LDH with CO_3^{2-}, NO_3^- and graphene inserted in between the layers, (B) XRD patterns, XPS (C) wide scan, (D) core level Ni 2p spectra of NiAl LDH/G LBL assembly.

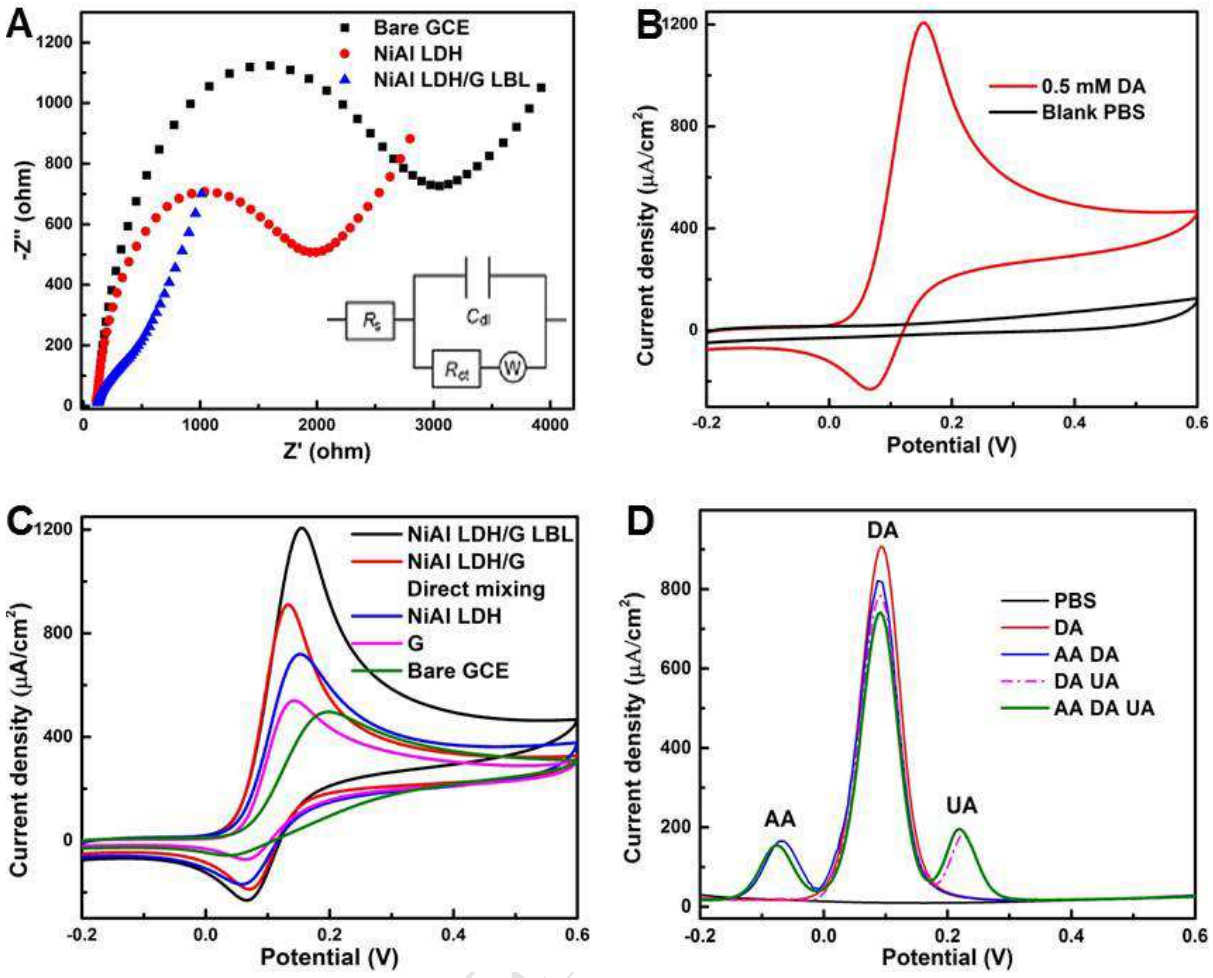

Fig. 4. (A) EIS plots of bare GCE and modified with NiAl LDH and NiAl LDH/G LBL in 0.1 M KCl containing 1.0 mM $K_3Fe(CN)_6$ and 1.0 mM $K_4Fe(CN)_6$. Frequency range: 0.1–105Hz. Inset is the equivalent circuit, (B) typical CV curves in the absence (black line) and presence (red line) of 0.5 mM DA in 0.1 M PBS (pH=7.4, scan rate=100 mV/s), (C) CV curves in the presence of 0.5 mM DA in 0.1 M PBS (pH=7.4) with different modified GCE, and (D) DPV profiles of DA between -0.2 V and 0.6 V *vs* SCE in the presence of different concentrations of AA and UA. DPV conditions: Incr E 4 mV, Amplitude 50 mV, Pulse width 0.06 s, Sample width 0.02 s, Pulse period 0.25 s, and Quiet time 2 s, (The number of experiments performed, n=6).

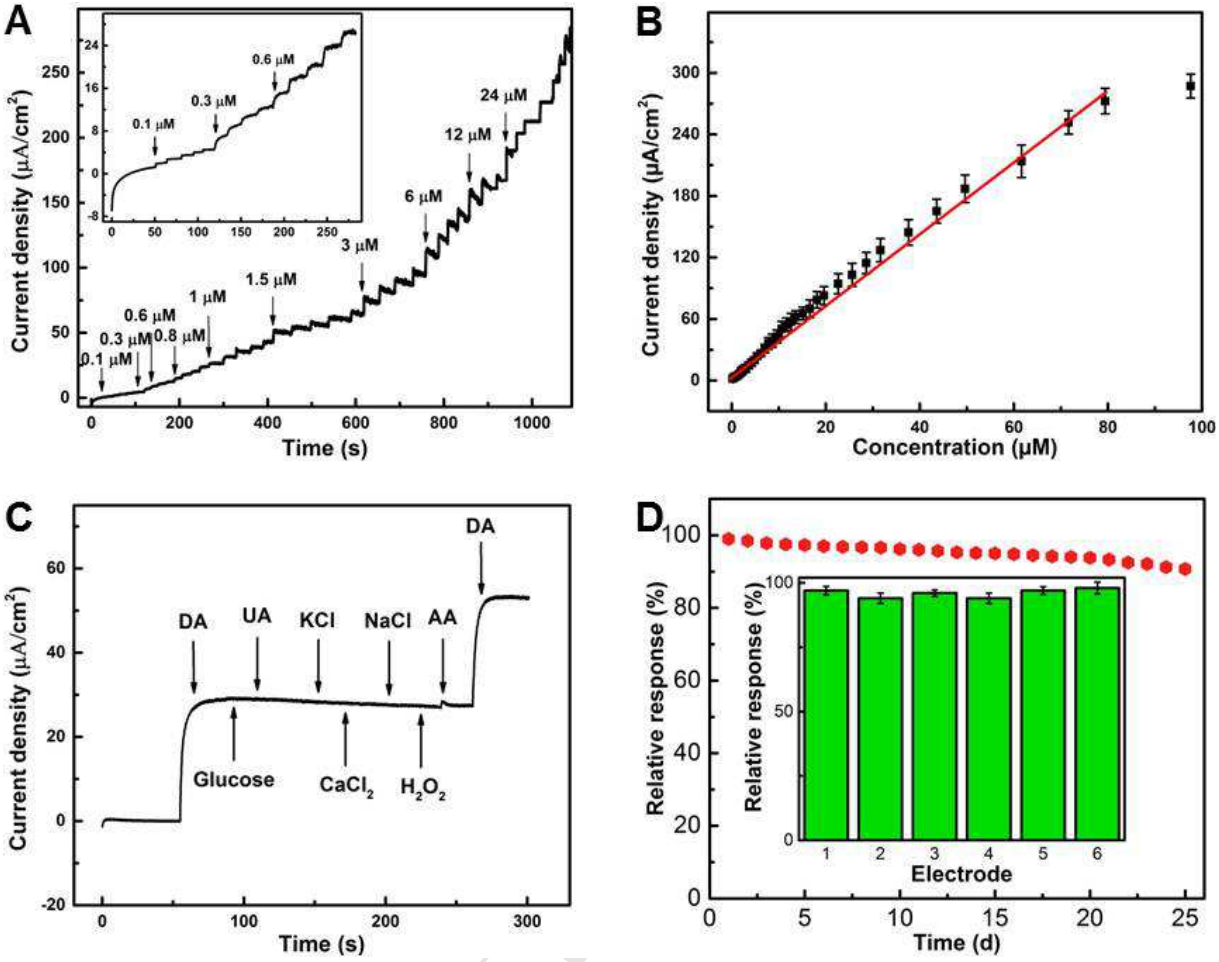

630

631 **Fig. 5.** (A) Amperometric i-t curve of NiAl LDH/G LBL electrode with successive additions of
632 different DA concentrations in N_2 saturated stirring 0.1 M PBS at an applied potential of 0.15 V.
633 (B) The linear calibration curve of current density *vs.* DA concentration, (C) Investigation of
634 interference activities on the response of 10 μM DA, and (D) Variation of current response to 0.5
635 mM DA with time. Inset is the current response of six different GC electrodes to 0.5 mM DA at
636 an applied potential of 0.14V, (n=6).

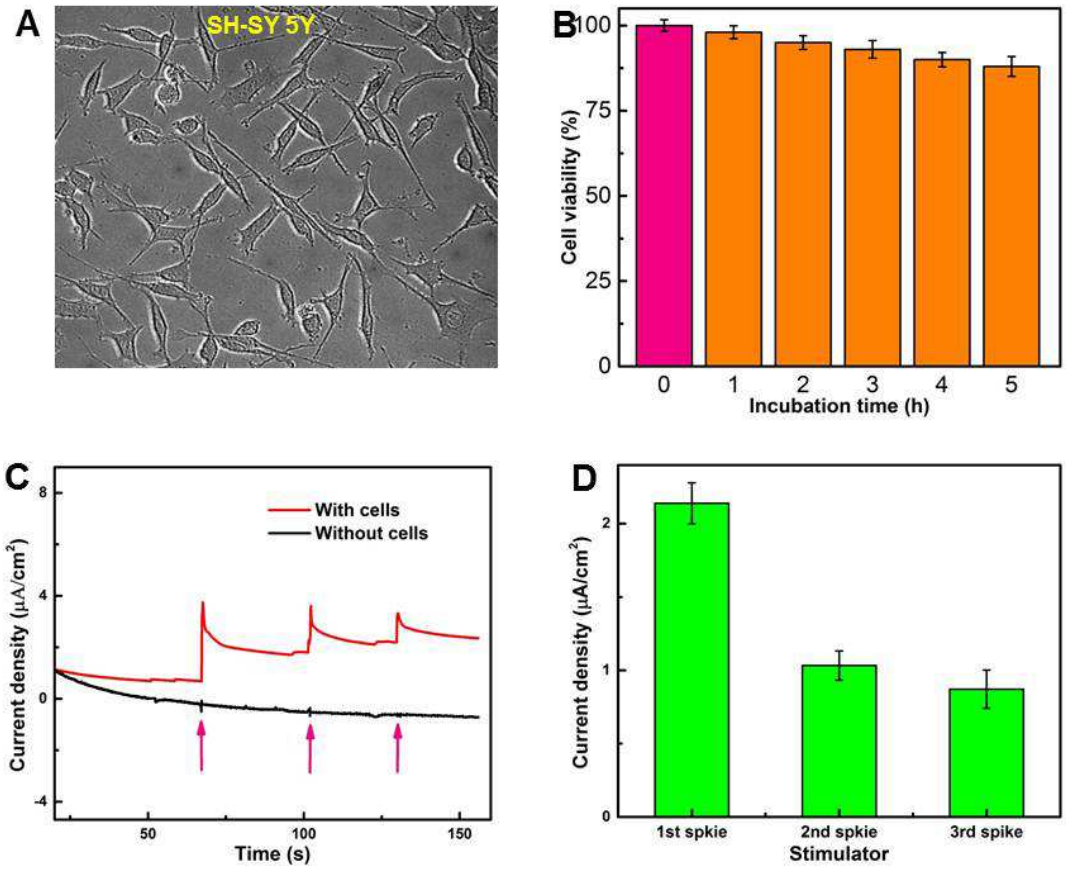

637

638 **Fig. 6.** (A) Bright-field image of neuroblastoma cell line, (B) Cell viability results performed by
639 CCK-8360 assay for SH-SY 5Y cells incubated with NiAl LDH/G LBL electrode (C)
640 Amperometric responses of NiAl LDH/G LBL electrode with the addition of different aliquots of
641 stimulator in the absence (black line) and presence (red line) of neuroblastoma cell line, and (D)
642 Analysis of current responses upon inoculation of different spikes of stimulator to living cells,
643 (n=6).

644

645

Highlights

- Optimized co-feeding methodology has been used for the fabrication of NiAl LDH/G LBL nanocomposites.
- Graphene nanosheets as π-electron-rich substrate modulate electronic structure of NiAl LDHs.
- NiAl LDH/G electrode exhibits excellent electrochemical performance for the sensitive detection of DA.
- Real-time monitoring of DA secretions from live human nerve cells.